Ultrafast dynamics of indirect exchange interaction and transient spin current generation in a two-dimensional electron gas

V. A. Stephanovich,[1,*] V. K. Dugaev,[2] V. I. Litvinov,[3] and J. Berakdar[4]

[1]*Institute of Physics, Opole University, 45-052 Opole, Poland*

[2]*Department of Physics and Medical Engineering, Rzeszów University of Technology, al. Powstańców Warszawy 6, 35-959 Rzeszów, Poland*

[3]*Sierra Nevada Corporation, 15245 Alton Parkway, Suite 100, Irvine, California 92618, USA*

[4]*Institut für Physik, Martin-Luther-Universität Halle-Wittenberg, Karl-Freiherr-von-Fritsch-Strasse 3, 06120 Halle (Saale), Germany*

(Received 10 October 2016; revised manuscript received 5 January 2017; published 24 January 2017)

We predict that a driven localized magnetic moment coupled to mobile carriers of a metal or semiconductor surface or interface generates a specific dynamics of the carrier spin density as well as a transient spin current. Numerical results illustrate the time-dependent Friedel oscillations and the associated ultrafast Ruderman-Kittel-Kasuya-Yosida (RKKY) interaction as well as the spin current generated by the impurity spin flipping. Retardation effects of the indirect exchange interaction of the impurity spins via the conduction electrons are found and discussed. Our results point to an alternative way of controlling the local magnetization on a subpicosecond time scale via appropriate tuning of the external fields that drive the magnetic dynamics of a localized moment.

DOI: 10.1103/PhysRevB.95.045307

I. INTRODUCTION

In the contemporary era of spintronics, the study of subpicosecond dynamics of impurity spins localized on metal and semiconductor surfaces and interfaces is becoming increasingly important. The surface spin dynamics provides a new platform to probe the interaction of localized spins with a two-dimensional (2D) electronic subsystem, which is utilizable for various spintronic applications such as memory devices [1], quantum gates [2], 2D spin field-effect transistors, light-emitting diodes, etc. [3]. A further application is the spin pumping across the interface between ferromagnetic and normal metals [4]. Manipulation of the spin state of a single on-surface paramagnetic impurity can be achieved with a terahertz (THz) pulse [5–7] by using all-electric means such as a tunneling tip in the scanning tunneling microscopy (STM) setup [8,9] or the gated channel in a Si-based field-effect transistor [9].

The indirect exchange interaction, mediated by near-surface electrons, couples localized spins and facilitates a spatial spin transfer (spin current) once the local spin switches its direction [4,10,11]. Thus, the spin density generated by dynamic impurity in a 2D electron gas acts on other magnetic moments, and their collective dynamics can be described phenomenologically by the Landau-Lifshitz-Gilbert (LLG) equation (see Ref. [1] for a review). In studies of spin-reversal processes, the dynamic Ruderman-Kittel-Kasuya-Yosida (RKKY) interaction [4,12–14] and the phenomenological (so-called micromagnetic) approach based on the LLG equation have been used to describe fast spin switching and subsequent magnetic relaxation. An underlying assumption is the separation of time scales: The magnetic relaxation is governed by the LLG dynamics on picosecond and longer time scales [5,15], while femtosecond processes should be treated microscopically (quantum mechanically) considering individual impurities based on a dynamic RKKY interaction. This problem has already been discussed in several articles related to the electronic properties of some metals, semiconductors [16,17], and, most recently, graphene [18–21].

To date, the dynamic RKKY interaction has been treated mostly in a frequency domain where it describes the response to a periodic-in-time spin perturbation [11–13,16,22,23]. However, various experimental conditions deal with an abrupt (pulsed) spin reversal necessitating a time-domain analysis, which is done in this paper. We study the dynamics of the spin polarization and the spin current generated by a fast reversal of a single-impurity spin $\mathbf{S}_0(t)$ coupled to a 2D electron gas of a host via *s-d* interaction. The electron gas becomes magnetically polarized, resulting in a time-dependent Friedel oscillations of the electron spin density $\mathbf{s}(\mathbf{r},t)$ around the localized spin (spin-density waves). The spatial and temporal evolution of the electron spin density and the spin current are calculated as they depend on the impurity spin-flip rate. Our primary goal here is to study the possibility to generate propagating spin density and spin current in 2D structures by dynamically manipulating the localized impurity moments.

II. TIME-DEPENDENT FRIEDEL OSCILLATIONS OF THE SPIN POLARIZATION AROUND DYNAMICAL IMPURITY SPIN

We begin with the standard Hamiltonian of the *s-d* exchange interaction between the dynamic magnetic impurity with spin $\mathbf{S}_0(t)$ located at $\mathbf{r} = 0$ and a 2D electron gas of a host crystal,

$$\mathcal{H}_{sd} = -\frac{\hbar^2\Delta}{2m^*} + \frac{g}{n}\,\delta(\mathbf{r})\,\sigma\cdot\mathbf{S_0}(t), \tag{1}$$

where Δ is the 2D Laplace operator, $n = N/A$ is the sheet density of the host atoms, g is the coupling constant, and σ is the vector of the Pauli matrices. We assume that the spin $\mathbf{S}_0(t)$ can be described classically. The Hamiltonian (1) describes the exchange coupling of the spins of 2D electron gas with a single-impurity spin $\mathbf{S}_0(t)$ which varies its orientation with time. This variation can be represented by spin rotation around a certain axis within some time interval. The rotation can be

*stef@uni.opole.pl

experimentally arranged by a terahertz pulse or by locally applied magnetic field in the STM setup.

Due to the magnetic coupling of the electrons and localized moment $\mathbf{S}_0(t)$, Friedel oscillations of 2D electron spin density $\mathbf{s}(\mathbf{r},t)$ develop around the localized spin. To obtain the response of 2D electron gas to the impurity spin flip we will use the perturbation theory in the coupling constant g. In the lowest order of perturbation theory we find the time-dependent distribution of spin polarization $\mathbf{s}(\mathbf{r},t)$ at a distance $\mathbf{r}$ from $\mathbf{S}_0(t)$,

$$s_\mu(\mathbf{r},t) = -\frac{ig}{\hbar}\,\mathrm{Tr}\int_{-\infty}^{t} dt'\,\sigma_\mu\,G_0(\mathbf{r},t;0,t')\,\sigma_\nu \times S_{0\nu}(t')\,G_0(0,t';\mathbf{r},t), \tag{2}$$

where $\mu,\nu = x,y,z$, Tr means the trace over the spin indices, and $G_0(\mathbf{r},t;\mathbf{r}',t')$ is the Green's function of unperturbed Hamiltonian (1), i.e., its first term [24],

$$G_0(\mathbf{r},t;\mathbf{r}',t') = \int \frac{d^2\mathbf{k}}{(2\pi)^2 n}\int_{-\infty}^{\infty}\frac{d\varepsilon}{2\pi} \times \frac{e^{i\mathbf{k}\cdot(\mathbf{r}-\mathbf{r}')}e^{-i\varepsilon(t-t')/\hbar}}{\varepsilon-\varepsilon_k+\varepsilon_F+i\Gamma\,\mathrm{sgn}\,\varepsilon}, \tag{3}$$

where $\varepsilon_k = \hbar^2k^2/2m^*$ (m^* is the electron effective mass), $\varepsilon_F = \hbar^2k_F^2/2m^*$ is the Fermi energy (accordingly, k_F is the Fermi momentum), and $\Gamma = \hbar/2\tau$ is the electron relaxation rate (accordingly, τ is the momentum relaxation time) related to the scattering of electrons from nonmagnetic impurities or defects.

Calculating in Eq. (3) the integrals over ε and the angle between vectors $\mathbf{k}$ and $\mathbf{r}-\mathbf{r}'$, we find

$$G_0(\mathbf{r},t;\mathbf{r}',t') = -\frac{ie^{i\varepsilon_F(t-t')/\hbar}}{2\pi n}\int_{k_F}^{\infty} kdk\,J_0(k|\mathbf{r}-\mathbf{r}'|) \times e^{-i(\varepsilon_k-i\Gamma)(t-t')/\hbar}, \quad t>t', \tag{4}$$

$$G_0(\mathbf{r},t;\mathbf{r}',t') = \frac{ie^{i\varepsilon_F(t-t')}}{2\pi n}\int_{0}^{k_F} kdk\,J_0(k|\mathbf{r}-\mathbf{r}'|) \times e^{-i(\varepsilon_k+i\Gamma)(t-t')/\hbar}, \quad t<t', \tag{5}$$

where $J_0(x)$ is the Bessel function [25].

Substituting Eqs. (4) and (5) in Eq. (2) and calculating the trace of Pauli matrices, we obtain

$$s_\mu(\mathbf{r},t) = -\frac{ig}{4\pi^2n^2\hbar}\int_{-\infty}^{t} dt'\,S_{0\mu}(t')\int_{k_F}^{\infty} kdk \times J_0(kr)\int_0^{k_F} k'dk'\,J_0(k'r)\,e^{-i(\varepsilon_k-\varepsilon_{k'}-2i\Gamma)(t-t')/\hbar}. \tag{6}$$

Expression (6) defines the magnetic response of a 2D electron gas to the time-dependent perturbation $S_{0\mu}(t)$.

Now we consider the experimentally relevant case when $\mathbf{S}_0(t)$ switches from an orientation along the z axis to the opposite direction by rotating around the x axis. This means that its y component is time dependent with the following parametrization:

$$S_{0y}(t) = \begin{cases}\tilde{S}_0\cos(\pi t/T), & |t|<T/2,\\ 0, & |t|\geqslant T/2,\end{cases} \tag{7}$$

corresponding to uniform rotation of vector $\mathbf{S}_0$. Here T is the spin-flip time. Using Eqs. (6) and (7), we obtain

$$s_y(\mathbf{r},t) = -\frac{ig\tilde{S}_0}{4\pi^2n^2\hbar}\int_{-T/2}^{\min\{t,\,T/2\}} dt'\,\cos\left(\frac{\pi t'}{T}\right) \times\int_{k_F}^{\infty} kdk\,J_0(kr)\int_0^{k_F} k'dk'\,J_0(k'r) \times e^{-i(\varepsilon_k-\varepsilon_{k'}-2i\Gamma)(t-t')/\hbar}. \tag{8}$$

For a very large time of spin flip, $T\to\infty$ (more exactly, if the spin-flip time T is longer than the electron relaxation time τ and also $T\gg t$), it follows from (8) that $s_y(\mathbf{r},t)$ becomes time independent,

$$s_y(\mathbf{r},T\to\infty) \simeq -\frac{ig\tilde{S}_0}{4\pi^2n^2}\int_{k_F}^{\infty} kdk\,J_0(kr) \times\int_0^{k_F} k'dk'\,\frac{J_0(k'r)}{\varepsilon_k-\varepsilon_{k'}-2i\Gamma}. \tag{9}$$

The integrals in Eq. (9) can be evaluated exactly in the case of $\Gamma\to 0$ (static spin polarization has already relaxed, so that in this case $\tau\to\infty$). Taking the limit of $\Gamma\to 0$ in (9) and expressing the integral from k_F to ∞ as a difference of integrals from zero to ∞ and from zero to k_F allow us to obtain a linear equation for the integrals in (9), which yields finally the ordinary RKKY result (see, e.g., Refs. [26–28]) for the static single spin $\mathbf{S}_0$ in a 2D electron gas,

$$s_y(\mathbf{r}) \simeq -\frac{gm^*k_F^2\tilde{S}_0}{8\pi n^2\hbar^2}[J_0(k_Fr)\,N_0(k_Fr)+J_1(k_Fr)\,N_1(k_Fr)], \tag{10}$$

where $N_0(z)$ and $N_1(z)$ are the Neumann functions [25].

To calculate the 2D electron gas response (8) numerically, we can express, similar to the static case, the integral from k_F to ∞ via those from zero to ∞ and from zero to k_F. This procedure yields the following result:

$$s_y(z,t_0) = -s_{y0}\int_a^{t_0+T_0/2}\cos\frac{\pi(t_0-x)}{T_0}e^{-x/\tau_0}dx \times\int_0^{\infty} y_1J_0(y_1z)dy_1\int_0^1 yJ_0(yz) \times\sin\left[x\left(y_1^2-y^2\right)\right], \tag{11}$$

where $a=0$ if $t_0<T_0/2$ and $a=t_0-T_0/2$ if $t_0>T_0/2$, $s_{y0} = gk_F^4\tilde{S}_0/(4\pi^2\varepsilon_Fn^2)$, $\varepsilon_F(t-t')/\hbar = x$, $y = k/k_F$, $y_1 = k'/k_F$, $t_0 = \varepsilon_Ft/\hbar$, $\tau_0 = \varepsilon_F\tau/\hbar$, $T_0 = \varepsilon_FT/\hbar$.

The spatial dependence of RKKY-type spin density is shown in Fig. 1 at different dimensionless running times t_0 for different spin-flip times T_0. The choice of parameters has been dictated by the experimental situation in fast optical switching on a femtosecond time frame: 80 fs [15] and 60 and 12 fs [6]. The shortest pulse corresponds to $T_0 = 20$ ($\varepsilon_F = 1$ eV) or $T_0 = 2$ ($\varepsilon_F = 0.1$ eV). Electron momentum relaxation time is in picoseconds, so below we use $\tau_0 = 100$.

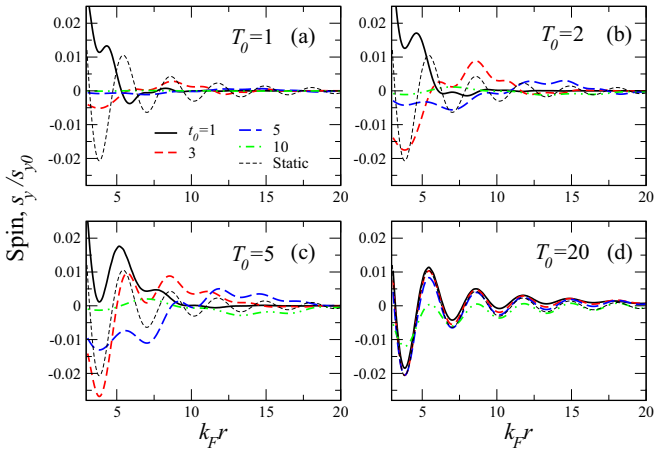

FIG. 1. Spin-density oscillations at different dimensionless times t_0 [as explained in the legend in (a)]. (a)–(d) show different choices of T_0, as shown in each panel. Dimensionless relaxation time $\tau_0 = 100$.

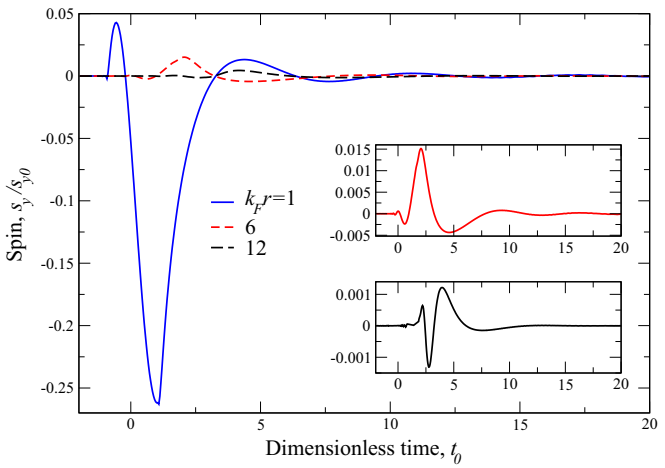

FIG. 3. Time dependences of spin polarization taken at different spatial points, shown in the legend. Insets visualize the temporal behavior of the curves for $k_F r = 6$ (top) and $k_F r = 12$ (bottom). The curves are plotted for $T_0 = 2$ and $\tau_0 = 100$.

It is seen in Fig. 1 that at small T_0 [Figs. 1(a) and 1(b)] the spatial spin distributions differ strongly from the static curve (10) and have irregular oscillatory behavior, while the curves for $T_0 = 20$ [Fig. 1(d)] follow the static one, especially at small $t_0 < T_0/2$. This behavior is also seen in Fig. 1(c), where an intermediate regime of $T_0 = 5$ is depicted. Also, at smaller T_0 the amplitude of system response is higher and decays drastically at elevated times. The main factor here is the relation between running time t_0 and the time of external spin flip T_0. Namely, at $t_0 < T_0/2$ the amplitude of the response is high, and spatial (Friedel) oscillations are irregular. In the opposite case, $t_0 < T_0/2$, the oscillations become more regular and approach the static regime at large enough $T_0 = 20$. Note that the irregular oscillatory behavior in the curves corresponding to $T_0 < 20$ is due to the fact that the time response of the system to the localized spin flip (7) "spoils" regular Friedel oscillations, given by Eq. (10).

The behavior in Fig. 1 is further visualized in Fig. 2, where the spin-flip time T_0 is now the parameter. In can be seen

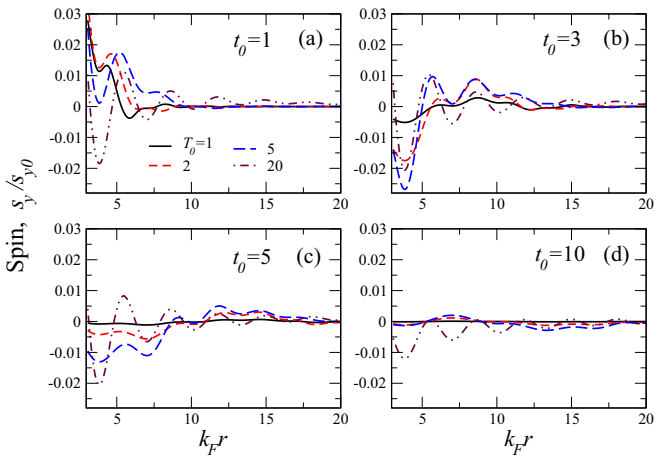

FIG. 2. Spin-density oscillations for different spin-flip times T_0, as explained in the legend in (a). (a)–(d) show different values of t_0. Dimensionless relaxation time $\tau_0 = 100$.

that when T_0 increases, the spin-density oscillations become increasingly more regular. At the same time, at larger time instants t_0, the spin amplitude decreases substantially, which is seen in Figs. 2(a)–2(d). Also, at large $k_F r$ the spin density decays quickly, which is especially true for small T_0. The nonmonotonic dependence on T_0 can also be observed: At $t_0 = 1$ the curve with $T_0 = 1$ has the highest amplitude at moderate $k_F r < 5$, while this curve has the smallest amplitude for $t_0 = 5$ and 10. At large $t_0 = 10$ [Fig. 2(d)] the highest amplitude is for the curve for $T_0 = 20$, which once more demonstrates the dependence of the system response on the ratio t_0/T_0.

The temporal evolution of the spin density is shown in Fig. 3. As the amplitude of the system response is much smaller at $z = k_F r = 6$ and 12, the details of corresponding curves are shown in the insets. The main effect here is the time lag in the system response as the distance from the source (magnetic impurity spin) grows. Indeed, while at $z = 1$ the maximal response occurs at $t_0 \approx 1$, at larger distances the maximal response amplitude (although it is much smaller than that at $z = 1$) occurs at $t_0 \approx 2.5$ ($z = 6$) and $t_0 \approx 4$ (positive pulse, $z = 12$). This demonstrates the retardation effect, when the system response appears earlier at a small distance from the impurity spin. The effect is clearly seen in Fig. 3 for $k_F r = 6$ and $k_F r = 12$. For a small distance, $k_F r = 1$, the retardation is very small but still exists.

III. SPIN CURRENT GENERATION BY IMPURITY SPIN REVERSAL

Now we are in a position to calculate the spin current, generated by the dynamical impurity spin. The spin current operator for our model has the form

$$\hat{J}_i^{\mu} = \frac{i\hbar}{2m^*}\left(\overleftarrow{\nabla}_i - \overrightarrow{\nabla}_i\right)\sigma_{\mu}, \tag{12}$$

where Latin indices refer to 2D coordinates in the x-y plane, $i = x, y$, and the arrows over operator ∇_i show the direction of the operator action. In our perturbation approach, the

expectation value of the spin current reads

$$J_i^{\mu}(\mathbf{r},t) = -\frac{g}{2m^*}\,\mathrm{Tr}\int_{-\infty}^{t} dt'\left(\frac{\partial}{\partial r_i}-\frac{\partial}{\partial r_i'}\right) \times \sigma_\mu\, G_0(\mathbf{r},t;0,t')\sigma_\nu\, S_{0\nu}(t')\, G_0(0,t';\mathbf{r}',t)\Big|_{\mathbf{r}=\mathbf{r}'}. \tag{13}$$

Substitution of expressions (4) and (5) for the Green's function yields the following explicit expression for the spin current:

$$J_i^{\mu}(\mathbf{r},t) = -\frac{g}{8\pi^2 m^*}\int_{-\infty}^{t} dt'\, S_{0\mu}(t')\left(\frac{\partial}{\partial r_i}-\frac{\partial}{\partial r_i'}\right) \times \int_{k_F}^{\infty} kdk J_0(kr)\int_0^{k_F} k'dk'\, J_0(k'r') \times e^{-i(\varepsilon_k-\varepsilon_{k'}-2i\Gamma)(t-t')/\hbar}\Big|_{\mathbf{r}=\mathbf{r}'}. \tag{14}$$

Calculating the derivatives of the Bessel functions and substituting expression (7) for $S_{0y}(t)$, we obtain

$$J_i^{y}(\mathbf{r},t) = \frac{r_i}{r}J^{y}(r,t), \tag{15}$$

where the coefficient $r_i/r = (x/r,\ \ y/r) = (\cos\varphi,\ \ \sin\varphi)$ signifies the angular part of the spin current (15). It appears from the derivative $\partial f(r)/\partial r_i = (r_i/r)(df/dr)$, where $f(r)$ is a function of only modulus $r = \sqrt{x^2+y^2}$. Thus, we call the term $J^y(r,t)$, which depends only on r, the *radial spin current*. In this case, the x and/or y components of spin current (15) are obtained by simply multiplying $J^y(r,t)$ by $\cos\varphi$ or $\sin\varphi$.

Then the explicit expression for radial spin current reads

$$J^{y}(r,t) = \frac{g\tilde{S}_0}{8\pi^2 m^* n^2}\int_{-T/2}^{\min\{t,T/2\}}[I_1(t-t')-I_2(t-t')] \times \cos\left(\frac{\pi t'}{T}\right)dt', \tag{16}$$

where

$$I_1(t-t') = \int_{k_F}^{\infty} k^2 dk\, J_1(kr) \times \int_0^{k_F} k'dk'\, J_0(k'r)\, e^{-i(\varepsilon_k-\varepsilon_{k'}-2i\Gamma)(t-t')/\hbar},$$

$$I_2(t-t') = \int_{k_F}^{\infty} kdk J_0(kr) \times \int_0^{k_F} k'^2 dk'\, J_1(k'r)\, e^{-i(\varepsilon_k-\varepsilon_{k'}-2i\Gamma)(t-t')/\hbar}.$$

Applying the above procedure, it is easy to show that in the static regime ($T\to\infty, \tau\to\infty$) the spin current is zero. This situation is opposite to that with the dynamic spin density. This means that there is no spin flow in thermodynamic equilibrium.

In dimensionless variables the radial spin current acquires the following form:

$$J^{y}(z,t_0) = J_0\int_a^{t_0+T_0/2}\cos\frac{\pi(t_0-x)}{T_0}e^{-x/\tau_0} \times [I_1(x,z)-I_2(x,z)]dx, \tag{17}$$

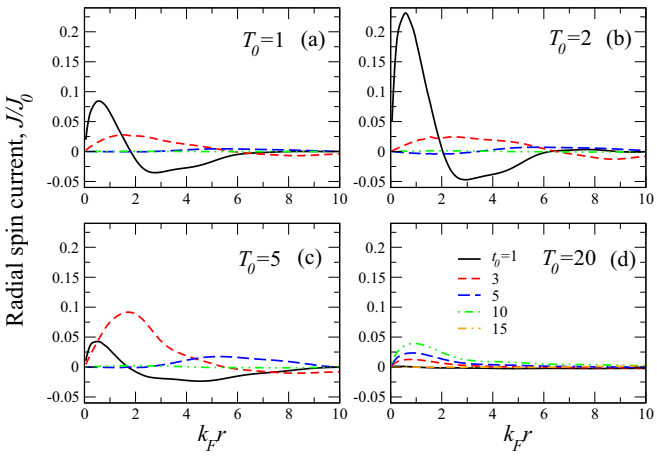

FIG. 4. Radial spin current Friedel oscillations at different dimensionless time instants t_0 [legend in (d)] and spin-flip times T_0. (a)–(d) show different T_0. Dimensionless relaxation time $\tau_0 = 100$.

with

$$I_1(x,z) = \int_0^{\infty} y^2 J_1(yz)dy \times \int_0^1 y_1 J_0(y_1 z)\cos\left[x\left(y_1^2-y^2\right)\right]dy_1,$$

$$I_2(x,z) = \int_0^{\infty} y J_0(yz)dy \times \int_0^1 y_1^2 J_1(y_1 z)\cos\left[x\left(y_1^2-y^2\right)\right]dy_1,$$

where we denote $J_0 = gk_F^5\hbar\tilde{S}_0/(8\pi^2 m^*\varepsilon_F n^2)$ and the rest of variables are similar to those in Eq. (11).

The spatial dependence of radial spin current is presented in Fig. 4 at different values of t_0 and T_0. Similar to the case of spin dynamics shown in Fig. 1, the physical picture here is determined by the interplay between t_0 and the spin-flip time T_0. Irregular oscillations are seen, similar to the case of dynamic spin response (Fig. 1). This means that the external spin flip not only generates the radial spin current but also spoils the regular Friedel oscillations in it. The nonmonotonic dependence on spin-flip time T_0 can be observed here. Really, for $t_0 = 1$ the maximal spin current amplitude occurs at $T_0 = 2$ [Fig. 4(b)], while for $t_0 = 3$ the maximal amplitude appears approximately at $T_0 = 5$ [Fig. 4(c)]. At both smaller and larger T_0 the spin current amplitude, corresponding to a specific time instant, is much less. At large $T_0 = 20$ (note the large relaxation time $\tau_0 = 100$) the spin current decays to zero, as has been discussed above.

In Fig. 5, we present the spatial dependence of the radial spin current but now the spin-flip time T_0 is the parameter. It can be seen that if T_0 increases, the amplitude of the spin current decays drastically. The same behavior occurs at larger times t_0: at $t_0 = 10$ the spin current is almost 50 times (except for the case of large $T_0 = 20$) less than that at $t_0 = 1$. At large distances, the radial spin current also decays quickly. The temporal evolution of the radial spin current is reported in Fig. 6. As the current amplitude is much smaller at $z = k_F r = 6$ and 12, the details are shown in the insets. Figure 6 illustrates

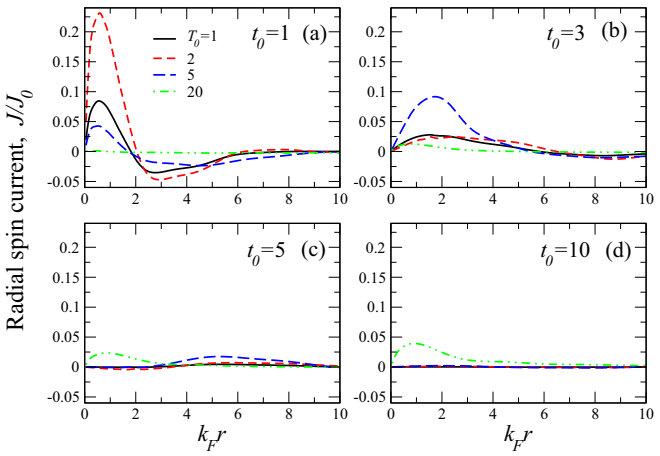

FIG. 5. Radial spin current Friedel oscillations plotted against spin-flip times T_0 [legend in (a)]. (a)–(d) show different t_0. Dimensionless relaxation time $\tau_0 = 100$.

the spin pumping that is clearly seen in the main panel at $k_Fr = 1$, where the spin current increases in time while the pulse lasts and then drops down after the pulse ends. Similar behavior is seen (although with a much smaller amplitude) in the insets with higher k_Fr. The retardation effect (see also Fig. 3) is also seen in the spin current. Namely, at larger distances from the local spin, the maximum spin current occurs at larger times t_0.

One more remark is needed here. When the impurity spin begins to rotate, the ambient 2D electron gas responds (after a time delay) by the difference in the local chemical potentials for spin-up and spin-down populations, which is indeed a spin accumulation effect. When the spin-up population prevails, we have a positive peak; otherwise, we have a negative one. As the spin accumulation peaks at $k_Fr = 1$ are already high, i.e., the majority of the electron spins are involved in them, for $k_Fr > 1$ the spin accumulation is accordingly low. The same effect has been observed experimentally and simulated

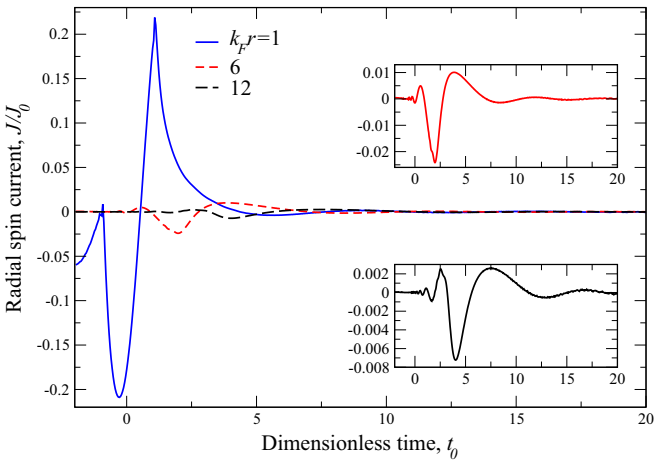

FIG. 6. Temporal evolution of radial spin current taken at different spatial points, shown in the legend. Insets visualize the temporal behavior of the curves for $k_Fr = 6$ (top) and $k_Fr = 12$ (bottom). The curves are plotted for $T_0 = 2$ and $\tau_0 = 100$.

by a simple phenomenological model of the spin diffusion in Ref. [29]. The close qualitative resemblance of Figs. 3(c) and 4(c) of Ref. [29] and our Figs. 3 and 6 is immediately seen.

IV. SUMMARY AND OUTLOOK

Although the indirect RKKY exchange interaction is well known in solid-state physics, this topic has become recurrent in the emergent field of ultrafast spintronics. As time- and spin-resolved spectroscopic tools become more sophisticated and available, the predicted effects should become accessible to experiment. For instance, in a recent work [30] the presence of a nonequilibrium spin current has been sensed by the emitted THz radiation. Our predicted spin currents can readily be detected by these new methods so that the anticipated power spectrum follows from the calculated time dependence of the spin currents.

Here, based on dynamic RKKY-type coupling in the time domain, we studied the temporal spin excitation and spin current evolution in a 2D electron gas. Our theoretical approach adequately describes spin excitation propagation after fast optical or all-electrical spin reversal on a 2D object like a metal and/or semiconductor surface as well as in a degenerate semiconductor inversion layer or interface.

Our approach complements the standard LLG theory for smaller (femtosecond) time scales, when phenomenological treatment of spin dynamics becomes inadequate. The results presented in this paper relate the femtosecond external pulse length to time and spatial propagation of the perturbation induced by a 2D RKKY interaction. We have shown that the system reaction to the local spin switching is retarded; that is, there is a time lag between impurity spin direction switching and system response in the form of local magnetization and/or spin current, which can clearly be observed at large distances. Our analysis shows that at chosen values of spin flip and electron relaxation times the charge-carrier concentration of $n_s = 10^{13}$ to 10^{14} cm^{-2}, typical for thin semiconducting films and inversion layers, is sufficient to observe experimentally the femtosecond magnetic response. Since the results are valid for a variety of 2D magnetic objects like adatoms, nanoparticles, and vacancy-induced magnetic moments on the semiconductor surface, this may open the path to new ways of transporting magnetic information in multilayer spintronic devices, which may be used in magnetic memory devices [1,3,21].

The spin-density excitation of electron gas generated by magnetic impurity (6) determines the dynamic exchange interaction of two magnetic impurities at a distance r. It can be an arbitrary pair of localized spins in magnetic semiconductors like GaMnAs [3]. The parameters of these host magnetic semiconductors (Fermi energy $E_F \simeq 30$ meV, heavy-hole mass $m \simeq 0.5m_0$, and average distance between impurities $r \simeq 10^{-6}$ cm) make it possible to observe clearly the dynamics of the above indirect exchange interaction for times $T \sim r/v_F \simeq 1$ ps. At the same time, the impurity spins are distributed chaotically in a semiconducting host, so that their separation is random. Therefore, to observe reliably the indirect exchange interaction dynamics it is necessary to use pairs of impurity spins (magnetic atoms) with an *a priori* given

distance between them. Also, they should be well separated from the environment.

Recently, a lot of attention has been attracted to "atom-by-atom engineered structures" of nanomagnets built from magnetic adatoms at the surface of nonmagnetic metal (see, for example, Ref. [31] and references therein). For example, they can be Fe or Co single atoms or clusters on the Cu(111) substrate. In the static case, the interaction between magnetic adatoms has the usual RKKY form [31–33]. The main advantage of the technology of such systems is the possibility of precise control of their parameters. As shown in Refs. [7,34], the dynamics of magnetic switching in these structures is also under consideration with switching times of 10 ns and distances $r \simeq 1$ nm. Taking the Fermi velocity for Cu $v_F \simeq 10^8$ cm/s, we find that a dynamical correction of 1% to the static RKKY could be observed at times $T \simeq 100$ fs, i.e., at much smaller switching times than those in the experiment of Ref. [7]. The related dynamics of a single spin switching in the experiment [34] has been theoretically analyzed in Ref. [35].

Therefore, we believe that the dynamical exchange interaction is much more important in structures with magnetic adatoms on a nonmagnetic semiconductor substrate. Namely, these structures permit us to measure experimentally both dynamic spin polarization and spin current, generated by the spin reversal of a magnetic adatom (like Fe, as in Ref. [35], or Mn), localized on the surface. For example, sandwich structures, fabricated in Ref. [29], can be equipped with the adatom on their surface as well as by the scanning tunneling microscopy tip to detect (in the spin-resolved case) the spin rotations and currents. The latter phenomena in this case are caused by the spin reversal of the magnetic adatom and can be measured for structures with different thicknesses of the Cu layer (see Ref. [29]), which mimics our $k_F r$ parameter. To observe the spin current it is more appropriate to use the standard technique of transversal electric current measurement with the inverse spin Hall effect. To do so, one can place nonmagnetic heavy-metal spin-orbit impurities (e.g., Au) at a distance from the rotated spin.

Using the above estimations we can also find the upper limit of the frequency of signals, which can be transmitted between magnetic atoms on the metallic surface at a distance of 1 nm. This frequency is about 1 THz, which corresponds to signals with a duration of 100 fs transferred with a periodicity of 1 ps. For shorter pulses the signal would be significantly distorted; instead of isolated pulses, the neighboring atom would receive some irregular oscillation packets like those presented in Fig. 3.

In this work we do not discuss possible experimental ways for very fast reversal of the localized spins. This problem has been discussed in numerous papers in relation to the possibility of ultrafast magnetic memory [36–39]. The main idea is to use a transverse-to-spin pulsed magnetic field so that the spin flip is due to free precession to the angle π. It turns out that this idea permits us to reach the picosecond spin flips in magnetic nanoparticles. The main parameters limiting such a macrospin rotation are related to magnetic anisotropy, the damping factor, and the temperature. Obviously, spin rotation of a free single adatom at the surface of a 2D nonmagnetic semiconductor should be much faster.

One can also use ultrafast laser excitation of an atom (molecule) with the corresponding change of its electronic state from the nonmagnetic to the magnetic one and back again from the excited magnetic state to the equilibrium nonmagnetic state. In this case we have to use the different [from that in Eq. (7)] parametrization of $S_0(t)$ in Eq. (6). For instance, it can be parametrized as $S_0(t) = \tilde{S}_0/\cosh^2(t/T)$, which does not change our results qualitatively.

ACKNOWLEDGMENTS

This work was supported by the National Science Center in Poland as a research project No. DEC-2012/06/M/ST3/00042 and by the German DAAD Project R02021255 PPP Polen.

[1] A. Kirilyuk, A. V. Kimel, and T. Rasing, Rev. Mod. Phys. **82**, 2731 (2010).
[2] Y. Rikitake and H. Imamura, Phys. Rev. B **72**, 033308 (2005).
[3] I. Žutić, J. Fabian, and S. Das Sarma, Rev. Mod. Phys. **76**, 323 (2004).
[4] M. V. Costache, M. Sladkov, S. M. Watts, C. H. van der Wal, and B. J. van Wees, Phys. Rev. Lett. **97**, 216603 (2006).
[5] S. Wienhold, D. Hinzke, and U. Novak, Phys. Rev. Lett. **108**, 247207 (2012).
[6] M. Battiato, K. Carva, and P. M. Oppeneer, Phys. Rev. Lett. **105**, 027203 (2010).
[7] S. Loth, S. Baumann, C. P. Lutz, D. M. Eigler, and A. J. Heinrich, Science **335**, 196 (2012).
[8] P. Berggren and J. Fransson, Sci. Rep. **6**, 25584 (2016).
[9] M. Xiao, I. Martin, E. Yablonovitch, and H. W. Jiang, Nature (London) **430**, 435 (2004).
[10] E. Šimánek and B. Heinrich, Phys. Rev. B **67**, 144418 (2003).
[11] G. M. Genkin, Phys. Rev. B **55**, 5631 (1997).
[12] J. Fransson, Phys. Rev. B **82**, 180411(R) (2010).
[13] S. R. Power, F. S. M. Guimaraes, A. T. Costa, R. B. Muniz, and M. S. Ferreira, Phys. Rev. B **85**, 195411 (2012).
[14] W. Chantrell, M. Wongsam, T. Schrefl, and J. Fidler, in *Encyclopedia of Materials: Science and Technology*, edited by K. H. J. Buschow, R. W. Cahn, M. C. Flemings, B. Ilschner, E. J. Kramer, and S. Mahajan (Elsevier, Amsterdam, 2001).
[15] G. Malinowski, F. Dalal Longa, J. H. H. Rietjens, P. V. Paluskar, R. Huijink, and H. J. M. Swagten, Nat. Phys. **4**, 855 (2008).
[16] S. Bhattacharjee, L. Nordström, and J. Fransson, Phys. Rev. Lett. **108**, 057204 (2012).
[17] M. R. Mahani, A. Pertsova, and C. M. Canali, Phys. Rev. B **90**, 245406 (2014).
[18] A. H. Castro Neto, F. Guinea, N. M. R. Peres, K. S. Novoselov, and A. K. Geim, Rev. Mod. Phys. **81**, 109 (2009).
[19] S. Das Sarma, S. Adam, E. H. Hwang, and E. Rossi, Rev. Mod. Phys. **83**, 407 (2011).
[20] V. K. Dugaev, V. I. Litvinov, and J. Barnaś, Phys. Rev. B **74**, 224438 (2006).
[21] X. Duan, V. A. Stephanovich, Y. G. Semenov, and K. W. Kim, Appl. Phys. Lett. **101**, 013103 (2012).

[22] J. Fransson, O. Eriksson, and A. V. Balatsky, Phys. Rev. B **81**, 115454 (2010).
[23] J. Fransson, J. Ren, and J. X. Zhu, Phys. Rev. Lett. **113**, 257201 (2014).
[24] E. M. Lifshitz and L. P. Pitaevskii, *Statistical Physics*, Part 2 (Pergamon, Oxford, 1980).
[25] *Handbook of Mathematical Functions*, edited by M. Abramowitz and I. I. Stegun, National Bureau of Standards Applied Mathematics Series 55 (National Bureau of Standards, Washington, DC, 1964).
[26] V. I. Litvinov and V. K. Dugaev, Phys. Rev. B **58**, 3584 (1998).
[27] B. Fisher and M. W. Klein, Phys. Rev. B **11**, 2025 (1975).
[28] M. T. Beal-Monod, Phys. Rev. B **36**, 8835 (1987).
[29] G.-M. Choi, B.-C. Min, K.-J. Lee, and D. G. Cahill, Nat. Commun. **5**, 4334 (2014).
[30] T. Seifert *et al.*, Nat. Photonics **10**, 483 (2016).
[31] A. A. Khajetoorians, J. Wiebe, B. Chilian, S. Lounis, S. Blügel, and R. Wiesendanger, Nat. Phys. **8**, 497 (2012).
[32] P. Wahl, P. Simon, L. Diekhöner, V. S. Stepanyuk, P. Bruno, M. A. Schneider, and K. Kern, Phys. Rev. Lett. **98**, 056601 (2007).
[33] H. Oka, P. A. Ignatiev, S. Wedekind, G. Rodary, L. Niebergall, V. S. Stepanyuk, D. Sander, and J. Kirschner, Science **327**, 843 (2010).
[34] S. Loth, M. Etzkorn, C. P. Lutz, D. M. Eigler, and A. J. Heinrich, Science **329**, 1628 (2010).
[35] M. Schüler, Y. Pavlyukh, and J. Berakdar, New J. Phys. **14**, 043027 (2012).
[36] C. H. Back, R. Allenspach, W. Weber, S. S. P. Parkin, D. Weller, E. L. Garwin, and H. C. Siegman, Science **285**, 864 (1999).
[37] M. Bauer, J. Fassbender, B. Hillebrands, and R. L. Stamps, Phys. Rev. B **61**, 3410 (2000).
[38] H. W. Schumacher, C. Chappert, R. C. Sousa, P. P. Freitas, and J. Miltat, Phys. Rev. Lett. **90**, 017204 (2003).
[39] A. Sukhov and J. Berakdar, Phys. Rev. Lett. **102**, 057204 (2009).